

**Beam energy dependence of Coulomb-nuclear interference in the breakup of  $^{11}\text{Be}$** 

R. Chatterjee\*

*Dipartimento di Fisica and INFN, Università di Padova, via F. Marzolo 8, I-35131 Padova, Italy*

(Received 14 February 2007; published 8 June 2007)

Within the post-form distorted wave Born approximation wherein pure Coulomb, pure nuclear and their interference terms are treated consistently in a single setup we study the beam energy dependence of the Coulomb-nuclear interference terms in the breakup of  $^{11}\text{Be}$  on a medium mass  $^{44}\text{Ti}$  target. Our results suggest that the Coulomb-nuclear interference terms are dependent on the incident beam energy and can be as big as that of the individual Coulomb or nuclear terms depending on the angle and energy of the breakup fragments. We also calculate the relative energy spectra and one-neutron removal cross sections in the breakup of  $^{11}\text{Be}$  on a heavy  $^{208}\text{Pb}$  target at 69 MeV/nucleon for two different angular ranges of the projectile center of the mass scattering angle and compare them with recently available experimental data.

DOI: [10.1103/PhysRevC.75.064604](https://doi.org/10.1103/PhysRevC.75.064604)

PACS number(s): 25.60.Gc, 24.10.Eq, 24.50.+g

**I. INTRODUCTION**

Nuclei away from the valley of stability have opened a new paradigm in nuclear physics. They are often extremely unstable (especially those closer to the drip lines) and have structure and properties which are quite often different from stable isotopes. Many of them exhibit a halo structure in their ground states in which loosely bound valence nucleon(s) has (have) a large spatial extension with respect to the respective core [1–4].

There have been several attempts, within a fully microscopic approach, to understand the stability of these weakly bound systems. A few of them, like different continuum shell model approaches [5,6], including the shell model embedded in the continuum [7,8], are formulated in the Hilbert space, i.e., they are based on the completeness of a single particle basis consisting of bound orbits and a real continuum. A different approach to the treatment of particle continuum is proposed in the Gamow shell model [9], which is the multiconfigurational shell model with a single particle basis given by the Berggren ensemble [10] consisting of Gamow (or resonant) states and the complex nonresonant continuum of scattering states. A microscopic cluster study of neutron rich carbon isotopes has also been performed with the generator coordinate method in Ref. [11]. However, a lot more needs to be done before one gets a more complete theoretical understanding of the underlying processes.

Another, widely used, method in unraveling the structure and properties of halo nuclei, is to use breakup reactions featuring the exotic projectile. For reviews of this ever burgeoning field from an experimental and theoretical perspective one is referred to Refs. [12] and [13], respectively. It is now abundantly clear that pure Coulomb [14–20] or pure nuclear [21–23] breakup calculations may not be fully sufficient to describe all the details of the halo breakup data which have been increasing rapidly both in quality and quantity [24–30]. In the majority of them both Coulomb and nuclear breakup effects as well as their interference terms are likely to be

significant and the neglect of the latter terms may not be justified [31–34]. The importance of nuclear effects even in the breakup of  $^8\text{B}$  in collisions with heavy ions has been discussed in Ref. [35]. Thus, an important requirement in interpreting the data obtained from the experiments done already or are planned to be done in future is to have a theory which can take care of the Coulomb and nuclear breakup effects as well as their interference terms on an equal footing.

For breakup reactions of light stable nuclei, such a theory has been developed [36] within the framework of post-form distorted wave Born approximation (DWBA), which successfully describes the corresponding data at low beam energies. However, since it uses the simplifying approximation of a zero-range interaction [37] between constituents of the projectile, it is inapplicable to cases where the internal orbital angular momentum of the projectile is different from zero.

Recently, we have presented a theory [38,39] to describe the breakup reactions of one-nucleon halo nuclei within the post-form DWBA (PFDWBA) framework, that consistently includes both Coulomb and nuclear interactions between the projectile fragments and the targets to all orders, but treats the fragment-fragment interaction in first order. The Coulomb and nuclear breakups along with their interference term are treated within a single setup in this theory. The breakup contributions from the entire continuum corresponding to all the multipoles and the relative orbital angular momenta between the valence nucleon and the core fragment are included in this theory where finite range effects are treated by a local momentum approximation (LMA) [40,41]. Full ground state wave function of the projectile, of any angular momentum structure, enters as an input to this theory.

The Coulomb-nuclear interference (CNI) terms have also been calculated using the prior-form DWBA [42] and within models [43,44] where the time evolution of the projectile in coordinate space is described by solving the time dependent Schrödinger equation, treating the projectile-target (both Coulomb and nuclear) interaction as a time dependent external perturbation. Recently, the dynamical eikonal method, which unifies the semiclassical time dependent and eikonal method and also takes into account interference effects has been used to calculate realistic differential cross sections [45,46]. Coulomb

\*rajdeep.chatterjee@pd.infn.it

and nuclear processes have also been treated consistently on the same footing, in the continuum discretized coupled-channels method [47–49] and also within an eikonal-like framework, in Refs. [50,51]. Nevertheless, to the best of our knowledge, the question of beam energy dependence of CNI has not been studied within breakup models before. Thus there is a need to address this question and investigate this new physics aspect within existing breakup theories itself, in view of several sophisticated experiments planned in the future.

In this paper, we investigate the beam energy dependence of the Coulomb-nuclear interference terms in the breakup of  $^{11}\text{Be}$  on a medium mass  $^{44}\text{Ti}$  target and also calculate the relative energy spectra and one-neutron removal cross sections in the breakup of  $^{11}\text{Be}$  on a heavy  $^{208}\text{Pb}$  target at 69 MeV/nucleon for two different angular ranges of the projectile center of the mass (c.m.) scattering angle. Our formalism is presented in Sec. II. In Sec. III, we present and discuss the results of our calculations for the breakup of  $^{11}\text{Be}$  on  $^{44}\text{Ti}$  and  $^{208}\text{Pb}$  targets. Summary and conclusions of our work are presented in Sec. IV.

## II. FORMALISM

We consider the elastic breakup reaction,  $a + t \rightarrow b + c + t$ , in which the projectile  $a$  ( $a = b + c$ ) breaks up into fragments  $b$  and  $c$  (both of which can be charged) in the Coulomb and nuclear fields of a target  $t$ . The triple differential cross section for this reaction is given by

$$\frac{d^3\sigma}{dE_b d\Omega_b d\Omega_c} = \frac{2\pi}{\hbar v_a} \rho(E_b, \Omega_b, \Omega_c) \sum_{\ell m} |\beta_{\ell m}|^2, \quad (1)$$

where  $v_a$  is the relative velocity of the projectile with respect to the target,  $\ell$  is the orbital angular momentum for the relative motion of  $b$  and  $c$  in the ground state of  $a$ , and  $\rho(E_b, \Omega_b, \Omega_c)$  is the appropriate phase space factor (see, e.g., Ref. [18]). The reduced transition amplitude, in Eq. (1),  $\beta_{\ell m}$  is defined as

$$\begin{aligned} \hat{\ell}\beta_{\ell m}(\mathbf{k}_b, \mathbf{k}_c; \mathbf{k}_a) &= \int d\mathbf{r}_1 d\mathbf{r}_i \chi_b^{(-)*}(\mathbf{k}_b, \mathbf{r}) \chi_c^{(-)*}(\mathbf{k}_c, \mathbf{r}_c) \\ &\times V_{bc}(\mathbf{r}_1) u_\ell(r_1) Y_m^\ell(\hat{r}_1) \chi_a^{(+)}(\mathbf{k}_a, \mathbf{r}_i), \end{aligned} \quad (2)$$

with  $\hat{\ell} \equiv \sqrt{2\ell + 1}$ . In Eq. (2), functions  $\chi_i$  represent the distorted waves for the relative motions of various particles in their respective channels with appropriate boundary conditions. The superscripts (+) and (−) represents outgoing and ingoing wave boundary conditions, respectively. Arguments of these functions contain the corresponding Jacobi momenta and coordinates.  $V_{bc}(\mathbf{r}_1)$  represents the interaction between  $b$  and  $c$ , and  $u_\ell(r_1)$  is the radial part of the corresponding wave function in the ground state of  $a$ . The position vectors (Jacobi coordinates) satisfy the relations (see also Fig. 1 of Ref. [18]):

$$\mathbf{r} = \mathbf{r}_i - \alpha \mathbf{r}_1, \quad \alpha = \frac{m_c}{m_c + m_b}, \quad (3)$$

$$\mathbf{r}_c = \gamma \mathbf{r}_1 + \delta \mathbf{r}_i, \quad \delta = \frac{m_t}{m_b + m_t}, \quad \gamma = (1 - \alpha\delta), \quad (4)$$

where  $m_i$  ( $i = a, b, c, t$ ) are the masses of various particles. In, what follows, we shall recollect only those formulas which are essential for our discussion. More details of the theory, especially those regarding the evaluation of  $\beta_{\ell m}$ , can be found in Ref. [39].

The reduced amplitude,  $\beta_{\ell m}$  [Eq. (2)], involves a six-dimensional integral which makes its evaluation quite complicated. The problem gets further aggravated due to the fact that the integrand involves the product of three scattering waves that exhibit an oscillatory behavior asymptotically. In order to facilitate an easier computation of Eq. (2), we perform a Taylor series expansion of the distorted waves of particles  $b$  and  $c$  about  $\mathbf{r}_i$  and write

$$\chi_b^{(-)}(\mathbf{k}_b, \mathbf{r}) = e^{-i\alpha \mathbf{K}_b \cdot \mathbf{r}_1} \chi_b^{(-)}(\mathbf{k}_b, \mathbf{r}_i), \quad (5)$$

$$\chi_c^{(-)}(\mathbf{k}_c, \mathbf{r}_c) = e^{i\gamma \mathbf{K}_c \cdot \mathbf{r}_1} \chi_c^{(-)}(\mathbf{k}_c, \delta \mathbf{r}_i). \quad (6)$$

Employing the LMA [40,41], the magnitudes of momenta  $\mathbf{K}_j$  are taken as

$$K_j(R) = \sqrt{(2m_j/\hbar^2)[E_j - V_j(R)]}, \quad (7)$$

where  $m_j$  ( $j = b, c$ ) is the reduced mass of the  $j$ - $t$  system,  $E_j$  is the energy of particle  $j$  relative to the target in the center of mass (c.m.) system, and  $V_j(R)$  is the potential between  $j$  and  $t$  at a distance  $R$ . Finally, one obtains

$$\begin{aligned} \hat{\ell}\beta_{\ell m} &= \frac{(4\pi)^3}{k_a k_b k_c \delta} i^{-\ell} Y_{m_\ell}^\ell(\hat{\mathbf{Q}}) Z_\ell(Q) \sum_{L_a L_b L_c} (i)^{L_a - L_b - L_c} \hat{L}_b \hat{L}_c \\ &\times \mathcal{Y}_{L_c}^{L_b}(\hat{k}_b, \hat{k}_c) \langle L_b 0 L_c 0 | L_a 0 \rangle \mathcal{R}_{L_b, L_c, L_a}(k_a, k_b, k_a), \end{aligned} \quad (8)$$

where

$$\mathcal{Y}_{L_c}^{L_b}(\hat{k}_b, \hat{k}_c) = \sum_M (-)^M \langle L_b M L_c - M | L_a 0 \rangle Y_M^{L_b}(\hat{k}_b) Y_M^{L_c}(\hat{k}_c), \quad (9)$$

$$Z_\ell(Q) = \int_0^\infty r_1^2 dr_1 j_\ell(Qr_1) u_\ell(r_1) V_{bc}(r_1), \quad (10)$$

$$\mathcal{R}_{L_b, L_c, L_a} = \int_0^\infty \frac{dr_i}{r_i} f_{L_a}(k_a, r_i) f_{L_b}(k_b, r_i) f_{L_c}(k_c, \delta r_i), \quad (11)$$

and  $\mathbf{Q} = \gamma \mathbf{K}_c - \alpha \mathbf{K}_b$ . In Eq. (11),  $f_{L_i}$  ( $i = a, b, c$ ) are the radial part of the partial wave ( $L_i$ ) expansion of distorted wave  $\chi_i^{(\pm)}$ , and is calculated by solving the Schrödinger equation with proper optical potentials which includes both Coulomb and nuclear terms. Generally, the maximum value of the partial waves  $L_a, L_b, L_c$  must be very large in order to ensure the convergence of the partial wave summations in Eq. (8). However, for the case of one-neutron halo nuclei, one can make use of the following method to include summations over infinite number of partial waves. We write  $\beta_{\ell m}$  as

$$\beta_{\ell m} = \sum_{L_i=0}^{L_i^{\max}} \hat{\beta}_{\ell m}(L_i) + \sum_{L_i=L_i^{\max}}^{\infty} \hat{\beta}_{\ell m}(L_i), \quad (12)$$

where  $\hat{\beta}$  is defined in the same way as Eq. (8) except for the summation sign and  $L_i$  corresponds to  $L_a$ ,  $L_b$ , and  $L_c$ . If the value of  $L_i^{\max}$  is chosen to be appropriately large, the contribution of the nuclear field to the second term of Eq. (12) can be neglected and we can write

$$\sum_{L_i=L_i^{\max}}^{\infty} \hat{\beta}_{\ell m}(L_i) \approx \sum_{L_i=0}^{\infty} \hat{\beta}_{\ell m}^{\text{Coul}}(L_i) - \sum_{L_i=0}^{L_i^{\max}} \hat{\beta}_{\ell m}^{\text{Coul}}(L_i), \quad (13)$$

where the first term on the right hand side, is the pure Coulomb breakup amplitude which for the case where one of the outgoing fragments is uncharged, can be expressed analytically in terms of the bremsstrahlung integral (see Ref. [18]). Therefore, only two terms, with reasonable upper limits, are required to be evaluated by the partial wave expansion in Eq. (12).

### III. CALCULATIONS ON $^{11}\text{Be}$

#### A. Structure model and optical potentials

The wave function,  $u_\ell(r)$ , appearing in the structure term,  $Z_\ell$  [Eq. (10)], has been calculated by adopting a single particle potential model in the same way as in Ref. [18,30]. The ground state of  $^{11}\text{Be}$  was considered to be a predominantly  $s$ -state with a  $2s_{1/2}$  valence neutron coupled to the  $0^+$   $^{10}\text{Be}$  core [ $^{10}\text{Be} \otimes 2s_{1/2}\nu$ ] with a one-neutron separation energy of 504 keV and a spectroscopic factor of 0.74 [52]. The single particle wave function was constructed by assuming the valence neutron- $^{10}\text{Be}$  interaction to be of Woods-Saxon type whose depth was adjusted to reproduce the corresponding value of the binding energy with fixed values of the radius and diffuseness parameters (taken to be 1.236 fm and 0.62 fm, respectively). This gave a potential depth of 59.08 MeV, a root mean square (rms) radius for the valence neutron of 7.07 fm, and a rms radius for  $^{11}\text{Be}$  of 2.98 fm when the size of the  $^{10}\text{Be}$  core was taken to be 2.28 fm. The neutron-target optical potentials used by us were extracted from the global set of Bechetti-Greenlees (see, e.g, [53]), while those used for the  $^{10}\text{Be}$ -target ([30,39]) system are shown in Table I. Following [43], we have used the sum of these two potentials for the  $^{11}\text{Be}$ -target channel. We found that values of  $L_i^{\max}$  of 500 and 400 for Pb and Ti targets, respectively, provided a very good convergence of the corresponding partial wave expansion series [Eq. (8)]. The local momentum wave vectors are evaluated at a distance,  $R = 10$  fm in all the cases, and their directions are taken to be same as that of asymptotic momenta. More details on the validity of this approximation can be found in the Appendix of Ref. [39].

#### B. Neutron energy distribution

It had been observed earlier that the CNI terms were dependent more on exclusive observables than on inclusive ones mainly due to the fact that multiply integrated quantities (theoretically) washed away the effect of interferences. Calculations of the double differential cross section (neutron energy

TABLE I. Optical potential parameters for the  $^{10}\text{Be}$ -target interaction. Radii are calculated with the  $r_j t^{1/3}$  convention.

System	$V_r$ (MeV)	$r_r$ (fm)	$a_r$ (fm)	$W_i$ (MeV)	$r_i$ (fm)	$a_i$ (fm)
$^{10}\text{Be}$ - $^{44}\text{Ti}$	70	2.5	0.5	10.0	1.5	0.50
$^{10}\text{Be}$ - $^{208}\text{Pb}$	50	1.45	0.8	57.9	1.45	0.8

distribution) for two forward neutron emission angles in the breakup of  $^{11}\text{Be}$  on Au at the beam energy of 41 MeV/nucleon, showed that the CNI terms were dependent on angles and energies of the outgoing neutron [39]. Their magnitudes were nearly equal to those of the nuclear breakup contributions which led to a difference in the incoherent and coherent sums of the Coulomb and nuclear contributions underlying thus the importance of those terms. In this subsection we shall present results of our calculations for the neutron energy distribution for the breakup of  $^{11}\text{Be}$  on a medium mass target at various beam energies and neutron emission angles ( $\theta_n$ ). In all these cases the core emission angle ( $\theta_{^{10}\text{Be}}$ ) is integrated from  $0^\circ$  to  $30^\circ$ .

In Fig. 1, we plot the neutron energy distribution for the breakup of  $^{11}\text{Be}$  on  $^{44}\text{Ti}$  at the low beam energy of 20 MeV/nucleon, for  $\theta_n = 1^\circ, 6^\circ, 11^\circ$ , and  $16^\circ$ . The dashed and dot-dashed lines represent the pure Coulomb and nuclear contributions, respectively, while total contributions are shown by solid lines. The plus signs and the inverted triangles represent the magnitudes of the positive and negative interference terms, respectively. At all neutron emission angles the Coulomb breakup terms are more than the nuclear ones at this low beam energy. We also see that the interferences at this beam energy

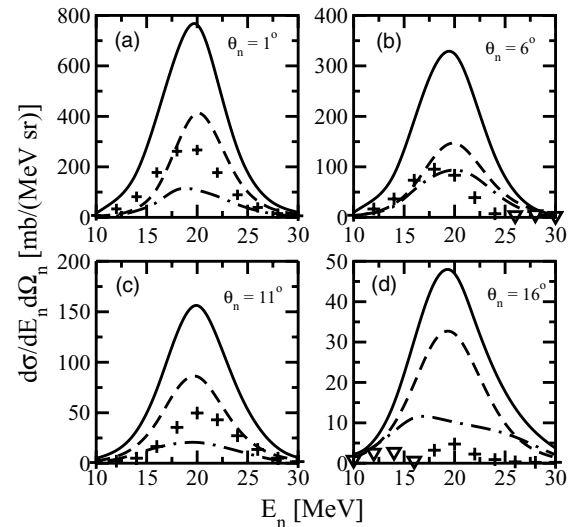


FIG. 1. Neutron energy distribution for the breakup reaction  $^{11}\text{Be}$  on  $^{44}\text{Ti}$  at the beam energy of 20 MeV/nucleon, for  $\theta_n = 1^\circ, 6^\circ, 11^\circ$ , and  $16^\circ$ . The dashed and dot-dashed lines represent the pure Coulomb and nuclear contributions, respectively, while total contributions are shown by solid lines. The plus signs and the inverted triangles represent the magnitudes of the positive and negative interference terms, respectively.

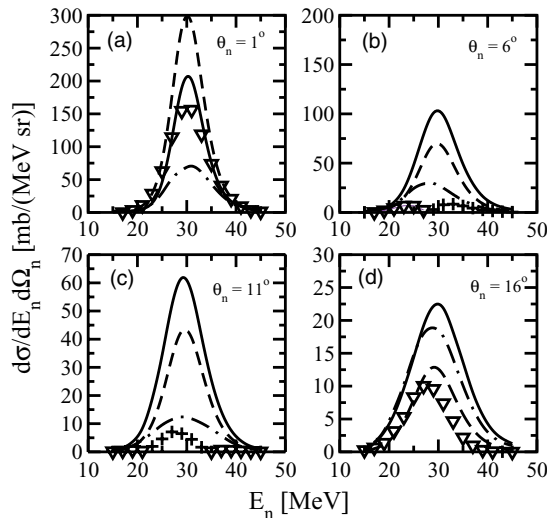


FIG. 2. Neutron energy distribution for the breakup reaction  $^{11}\text{Be}$  on  $^{44}\text{Ti}$  at the beam energy of 30 MeV/nucleon, for  $\theta_n = 1^\circ, 6^\circ, 11^\circ,$  and  $16^\circ$ . The dashed and dot-dashed lines represent the pure Coulomb and nuclear contributions, respectively, while total contributions are shown by solid lines. The plus signs and the inverted triangles represent the magnitudes of the positive and negative interference terms, respectively.

are constructive, in general, and that at the neutron angles of  $1^\circ$  and  $11^\circ$ , in Figs. 1(a) and 1(c), respectively, the magnitude of the interference terms are more than the nuclear terms for nearly all energies of the outgoing neutron.

A similar calculation performed at a higher beam energy is shown in Fig. 2, where we plot the neutron energy distribution for the breakup of  $^{11}\text{Be}$  on  $^{44}\text{Ti}$  at the beam energy of 30 MeV/nucleon, for  $\theta_n = 1^\circ, 6^\circ, 11^\circ,$  and  $16^\circ$ . Pure Coulomb and nuclear contributions are shown by dashed and dot-dashed lines, respectively, while total contributions are shown by solid lines. The plus signs and the inverted triangles represent the magnitudes of the positive and negative interference terms, respectively. At 30 MeV/nucleon, incident beam energy, we see that the Coulomb terms are larger than the nuclear ones at smaller neutron emission angles [Figs. 2(a)–2(c)], while at larger angles the nuclear part begins to dominate. The importance of the interference terms is highlighted in Fig. 2(a), where we see that the destructive interference terms not only cancel out the nuclear terms, but also reduces the Coulomb terms so that the coherent total sum is less than the Coulomb terms. At  $\theta_n = 16^\circ$  [Fig. 2(d)] we see that the destructive CNI terms nearly cancel out the Coulomb terms, especially from neutron energies of 15 MeV to 27 MeV, and the nuclear terms are sole contributors at these energies.

In Fig. 3, we plot the neutron energy distribution for the breakup of  $^{11}\text{Be}$  on  $^{44}\text{Ti}$  at the beam energy of 40 MeV/nucleon, for  $\theta_n = 1^\circ, 6^\circ, 11^\circ,$  and  $16^\circ$ . The dashed and dot-dashed lines represent the pure Coulomb and nuclear contributions, respectively, while total contributions are shown by solid lines. The plus signs and the inverted triangles represent the magnitudes of the positive and negative interference terms, respectively. We see that the Coulomb terms are larger than the nuclear ones at smaller neutron emission angles

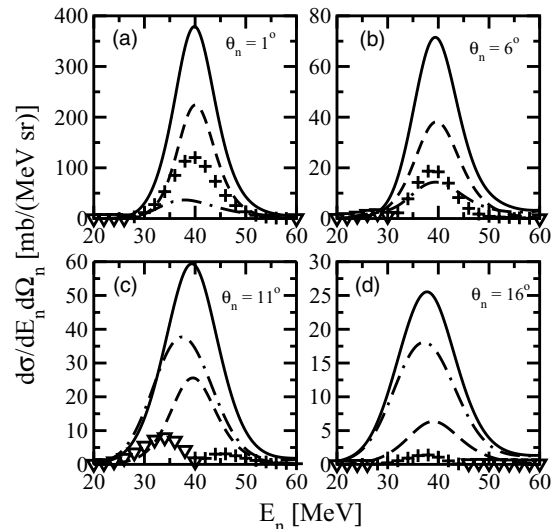


FIG. 3. Neutron energy distribution for the breakup reaction  $^{11}\text{Be}$  on  $^{44}\text{Ti}$  at the beam energy of 40 MeV/nucleon, for  $\theta_n = 1^\circ, 6^\circ, 11^\circ,$  and  $16^\circ$ . The dashed and dot-dashed lines represent the pure Coulomb and nuclear contributions, respectively, while total contributions are shown by solid lines. The plus signs and the inverted triangles represent the magnitudes of the positive and negative interference terms, respectively.

[Figs. 3(a), 3(b)], while at larger angles the nuclear part begins to dominate. The interference is generally constructive at smaller neutron angles, often being larger or almost equal to the individual nuclear terms ( $\theta_n = 1^\circ, 6^\circ$ ), while at  $\theta_n = 11^\circ$ , especially from neutron energies of 20 MeV to 35 MeV, the destructive CNI terms nearly cancel out the Coulomb terms, and the nuclear terms are sole contributors to the total cross section.

Our results, thus, indicate that the CNI terms are not only dependent on energies and angles of the outgoing fragments, they are also dependent on the incident beam energy. It would indeed be quite interesting if more exclusive cross section measurements could be made at low beam energies, where the effect of the CNI terms were found to be substantial, in a future experiment.

### C. Relative energy spectra

The relative energy spectrum of the fragments (neutron and  $^{10}\text{Be}$ ) emitted in the breakup of  $^{11}\text{Be}$  on  $^{208}\text{Pb}$  target at the beam energy of 69 MeV/nucleon is shown in Fig. 4, for different angular ranges of the projectile c.m. scattering angle ( $\theta_{at}$ ). The relative angle between the fragments ( $\theta_{n-^{10}\text{Be}}$ ) has been integrated from  $0^\circ$  to  $180^\circ$ . The dashed and dot-dashed lines represent the pure Coulomb and nuclear contributions, respectively, while total coherent contributions are shown by solid lines. The experimental data are from Ref. [30].

In the upper panel of Fig. 4,  $\theta_{at}$ -integration has been done in the range of  $0^\circ$ – $6^\circ$ . The pure Coulomb contributions dominate the cross sections around the peak value, while at larger relative energies the nuclear breakup is important. This was also observed in Refs. [39,43] and was attributed to the different energy dependence of the two contributions. In Ref. [39],

TABLE II. Total one-neutron removal cross section, various contributions from pure Coulomb and pure nuclear breakups, and their incoherent sum for  $^{11}\text{Be}$  breakup on  $^{208}\text{Pb}$ , at beam energy of 69 MeV/nucleon for two different angular ranges of  $\theta_{at}$ .

$\theta_{at}$ (deg.)	Total (b)	Pure Coulomb (b)	Pure nuclear (b)	Incoherent sum (b)	Expt. [30] (b)
$0^\circ\text{--}6^\circ$	1.534	1.191	0.367	1.558	$1.790 \pm 0.110(\text{syst}) \pm 0.020(\text{stat})$
$0^\circ\text{--}1.3^\circ$	0.489	0.484	0.005	0.489	—

however, the  $\theta_{at}$ -integration was done from  $0^\circ\text{--}40^\circ$  mainly to account for all nuclear contributions coming from small impact parameters.

The Coulomb breakup contribution has a long range and it shows a strong energy dependence. The number of virtual photons increases for small excitation energies and hence the cross sections rise sharply at low excitation energies. After a certain value of this energy the cross sections decrease due to setting in of the adiabatic cutoff. In contrast, the nuclear breakup occurs when the projectile and the target nuclei are close to each other. Its magnitude, which is determined mostly by the geometrical conditions, has a weak dependence on the relative energy of the outgoing fragments beyond a certain minimum value. The coherent sum of the Coulomb and nuclear contributions provides a good overall description of the experimental data.

The lower panel of Fig. 4, shows the relative energy spectra in which the  $\theta_{at}$ -integration was done from  $0^\circ\text{--}1.3^\circ$ . This is well below the grazing angle ( $=3.8^\circ$ ) for the reaction and consequently the Coulomb contribution in this case dominates over the nuclear part (which in fact is multiplied by a factor

of 10 to make it visible in the figure). Thus, the dashed and solid lines in the lower panel of Fig. 4, almost coincide with each other. This will also be reflected in the total one-neutron removal cross section which we present in the next sub section.

#### D. Total one-neutron removal cross section

In Table II, we show the contributions of pure Coulomb and pure nuclear breakup mechanisms to the total one-neutron removal cross sections in the breakup of  $^{11}\text{Be}$  on  $^{208}\text{Pb}$  for two different angular ranges of  $\theta_{at}$ , at the beam energy of 69 MeV/nucleon. The incoherent sum shown in the penultimate column of the table is obtained by simply adding the pure Coulomb and pure nuclear cross sections.

For the breakup of  $^{11}\text{Be}$  on Pb in the  $\theta_{at}$ -range of  $0^\circ\text{--}6^\circ$ , Coulomb breakup accounts for most ( $\approx 78\%$ ) of the total cross section, while in the angular range of  $0^\circ\text{--}1.3^\circ$  (well below the grazing angle) it accounts for almost all of the total cross section.

The total one-neutron removal cross section on Pb does not seem to be affected by the CNI terms. This is because the CNI terms manifest themselves explicitly in more exclusive measurements, like double differential cross sections than in quantities like total cross sections.

#### IV. SUMMARY AND CONCLUSIONS

In this paper, we have investigated the beam energy dependence of the Coulomb-nuclear interference terms in the breakup of  $^{11}\text{Be}$  on a medium mass  $^{44}\text{Ti}$  target and have also calculated the relative energy spectra for the breakup of  $^{11}\text{Be}$  on a heavy  $^{208}\text{Pb}$  target at 69 MeV/nucleon for two different angular ranges of the projectile center of the mass scattering angle. The calculations were performed within the fully quantum mechanical framework of post-form DWBA, where pure Coulomb, pure nuclear as well as their interference terms were treated consistently within the same framework. In this theory, both the Coulomb and nuclear interactions between the projectile and the target nucleus were treated to all orders, but the fragment-fragment interaction was treated in the first order. The full ground state wave function of the projectile corresponding to any orbital angular momentum structure enters as an input to this theory.

The exact post-form DWBA breakup amplitude was simplified with the LMA and the validity of the approximation was verified by calculating several reaction observables in the breakup of  $^{11}\text{Be}$  in the Coulomb and nuclear fields of several

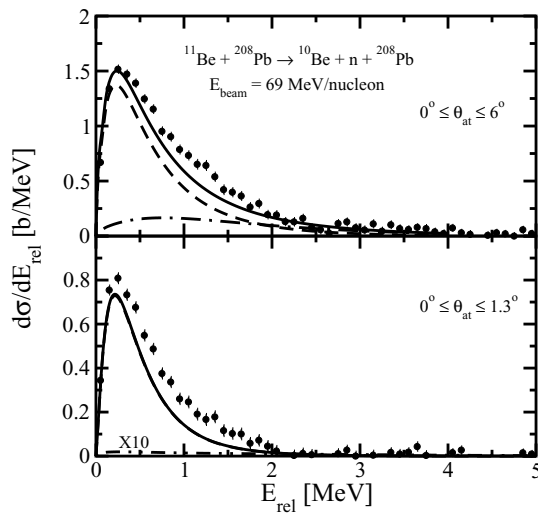


FIG. 4. Relative energy spectra for the breakup of  $^{11}\text{Be}$  on a  $^{208}\text{Pb}$  target at 69 MeV/nucleon, incident beam energy, for different angular ranges of  $\theta_{at}$ . The dashed and dot-dashed lines represent the pure Coulomb and nuclear breakup contributions, respectively, while total contributions are shown by solid lines. In the upper panel, integration over  $\theta_{at}$  has been done in the range of  $0^\circ\text{--}6^\circ$ , while in the lower panel  $\theta_{at}$  is integrated in the range of  $0^\circ\text{--}1.3^\circ$ . Experimental data are from Ref. [30]. For more details see the text.

targets, in different mass ranges, in Refs. [38,39]. Recently, there have been attempts to calculate the exact post-form DWBA without the LMA, for pure Coulomb breakup, with momentum space Coulomb wave functions [54]. While, this is indeed an welcome step, its practical applicability to calculate a wide variety of reaction observables is still an open question, particularly because it is numerically very intensive and time consuming. Thus the LMA still has practical applications, in this respect, particularly because along with its ability to factorise the Coulomb breakup amplitude it is also able to treat Coulomb and nuclear breakup on a single footing. Nevertheless, efforts are in progress [55] for the calculation of the post-form DWBA breakup amplitude without the LMA in a more analytic and less numerically intensive way than using momentum space Coulomb wave functions.

We calculated the neutron energy distributions for the breakup of  $^{11}\text{Be}$  on  $^{44}\text{Ti}$  at various beam energies and neutron emission angles. At 20 MeV/nucleon, beam energy, the Coulomb breakup accounted for more of the cross section than nuclear breakup and the CNI terms were constructive, in general. The importance of the CNI terms were again highlighted by the calculation at the beam energy of 30 MeV/nucleon, where the CNI terms at low neutron emission angles, not only cancel out the nuclear terms, but also reduces the Coulomb terms so that the coherent total sum is less than the Coulomb terms. At 40 MeV/nucleon, beam energy, interference was generally constructive at smaller neutron angles, often being larger or almost equal to the individual nuclear terms ( $\theta_n = 1^\circ, 6^\circ$ ), while at  $\theta_n = 11^\circ$ , especially from neutron energies of 20 MeV to 35 MeV, the destructive CNI terms nearly cancels out the Coulomb terms, and the nuclear terms are sole contributors to the total cross section. Our results, thus, indicate that the CNI terms are not only dependent on energies and angles of the outgoing fragments, they are also dependent on the incident beam energy. It would indeed be quite interesting if in a future experiment exclusive cross

section measurements could be made at low beam energies where the effect of the CNI terms were found to be substantial.

Calculations were also performed for the relative energy spectrum of the fragments (neutron and  $^{10}\text{Be}$ ) emitted in the breakup of  $^{11}\text{Be}$  on  $^{208}\text{Pb}$  target at the beam energy of 69 MeV/nucleon, for different angular ranges of the projectile c.m. scattering angle— $0^\circ$  to  $6^\circ$  and  $0^\circ$  to  $1.3^\circ$ . In the former angular range pure Coulomb contributions dominate the cross sections around the peak value, while at larger relative energies the nuclear breakup is important. In the latter range, which is well below the grazing angle, for the reaction Coulomb breakup dominates over the nuclear part.

The total one-neutron removal cross section was found not to be affected by the CNI terms as they manifest themselves explicitly in more exclusive measurements, like double differential cross sections than in quantities like total cross sections.

The full quantal theory of one-neutron halo breakup reactions, applied in this paper, can also be used to describe the  $(a, b\gamma)$  reaction provided the inelastic breakup mode is also calculated within this theory, which is expected to be straightforward. Furthermore, the theoretical method outlined in this paper rely on the nonrelativistic Schrödinger equation which in our opinion should be viewed only as an adequate starting point. There have been some attempts to use effective field methods to study halo nuclei [56]. This is indeed a very new field and would be quite interesting to pursue in view of experiments of halo breakup at very high beam energies for which data have been taken at GSI, Darmstadt.

#### ACKNOWLEDGMENTS

It is a pleasure to thank Prof. R. Shyam and Prof. A. Vitturi for many interesting discussions. Thanks, also to Prof. T. Nakamura for providing the experimental data shown in Fig. 4 in a tabular format.

- 
- [1] P. G. Hansen and B. M. Sherill, Nucl. Phys. **A693**, 133 (2001).
  - [2] I. Tanihata, Nucl. Phys. **A654**, 235c (1999); J. Phys. G **22**, 157 (1996).
  - [3] K. Riisager, Rev. Mod. Phys. **66**, 1105 (1994).
  - [4] C. A. Bertulani, L. F. Canto, and M. S. Hussain, Phys. Rep. **226**, 281 (1993).
  - [5] I. Rotter, Rep. Prog. Phys. **54**, 635 (1991).
  - [6] A. Volya and V. Zelevinsky, Phys. Rev. C **67**, 054322 (2003).
  - [7] J. Okołowicz, M. Płoszajczak, and I. Rotter, Phys. Rep. **374**, 271 (2003), and references therein.
  - [8] R. Chatterjee, J. Okołowicz, and M. Płoszajczak, Nucl. Phys. **A764**, 528 (2006).
  - [9] N. Michel, W. Nazarewicz, M. Płoszajczak, and K. Bennaceur, Phys. Rev. Lett. **89**, 042502 (2002).
  - [10] T. Berggren, Nucl. Phys. **A109**, 265 (1968); P. Lind, Phys. Rev. C **47**, 1903 (1993).
  - [11] P. Descouvemont, Nucl. Phys. **A675**, 559 (2000).
  - [12] B. Jonson, Phys. Rep. **389**, 1 (2004).
  - [13] G. Baur, K. Hencken, and D. Trautmann, Prog. Part. Nucl. Phys. **51**, 487 (2003).
  - [14] T. Nakamura *et al.*, Phys. Lett. **B331**, 296 (1994).
  - [15] T. Nakamura *et al.*, Phys. Rev. Lett. **83**, 1112 (1999).
  - [16] P. Banerjee, I. J. Thompson, and J. A. Tostevin, Phys. Rev. C **58**, 1042 (1998).
  - [17] P. Banerjee, J. A. Tostevin, and I. J. Thompson, Phys. Rev. C **58**, 1337 (1998).
  - [18] R. Chatterjee, P. Banerjee, and R. Shyam, Nucl. Phys. **A675**, 477 (2000).
  - [19] R. Chatterjee, P. Banerjee, and R. Shyam, Nucl. Phys. **A692**, 476 (2001).
  - [20] R. Chatterjee and P. Banerjee, Phys. Rev. C **63**, 017303 (2001).
  - [21] G. F. Bertsch, K. Hencken, and H. Esbensen, Phys. Rev. C **57**, 1366 (1998); H. Esbensen and G. F. Bertsch, *ibid.* **59**, 3240 (1999).
  - [22] A. Bonaccorso and F. Carstoiu, Phys. Rev. C **61**, 034605 (2000), and references therein.
  - [23] K. Yabana, Y. Ogawa, and Y. Suzuki, Nucl. Phys. **A539**, 295 (1992).
  - [24] P. G. Hansen, A. S. Jensen, and B. Jonson, Annu. Rev. Nucl. Part. Sci. **45**, 2 (1995).
  - [25] B. Davids *et al.*, Phys. Rev. Lett. **81**, 2209 (1998).
  - [26] D. Cortina-Gil *et al.*, Eur. Phys. J. A **10**, 49 (2001).

- [27] R. Kanungo *et al.*, Phys. Rev. Lett. **88**, 142502 (2002).  
[28] U. Datta Pramanik *et al.*, Phys. Lett. **B551**, 63 (2003).  
[29] R. Palit *et al.*, Phys. Rev. C **68**, 034318 (2003).  
[30] N. Fukuda *et al.*, Phys. Rev. C **70**, 054606 (2004).  
[31] R. Anne *et al.*, Phys. Lett. **B250**, 19 (1990).  
[32] R. Anne *et al.*, Nucl. Phys. **A575**, 125 (1994).  
[33] P. Banerjee and R. Shyam, Nucl. Phys. **A540**, 112 (1993);  
J. Phys. G **22**, L79 (1996).  
[34] V. Maddalena and R. Shyam, Phys. Rev. C **63**, 051601(R) (2001).  
[35] C. Dasso, S. M. Lenzi, and A. Vitturi, Nucl. Phys. **A639**, 635 (1998).  
[36] G. Baur, F. Rösler, D. Trautmann, and R. Shyam, Phys. Rep. **111**, 333 (1984).  
[37] G. R. Satchler, Nucl. Phys. **55**, 1 (1964).  
[38] R. Chatterjee and R. Shyam, Phys. Rev. C **66**, 061601(R) (2002).  
[39] R. Chatterjee, Phys. Rev. C **68**, 044604 (2003).  
[40] R. Shyam and M. A. Nagarajan, Ann. Phys. (NY) **163**, 285 (1985).  
[41] P. Braun-Munzinger and H. L. Harney, Nucl. Phys. **A233**, 381 (1974).  
[42] R. Shyam and I. J. Thompson, Phys. Rev. C **59**, 2645 (1999).  
[43] S. Typel and R. Shyam, Phys. Rev. C **64**, 024605 (2001).  
[44] J. Margueron, A. Bonaccorso, and D. M. Brink, Nucl. Phys. **A703**, 105 (2002).  
[45] D. Baye, P. Capel, and G. Goldstein, Phys. Rev. Lett. **95**, 082502 (2005).  
[46] G. Goldstein, D. Baye, and P. Capel, Phys. Rev. C **73**, 024602 (2006).  
[47] N. Austern *et al.*, Phys. Rep. **154**, 125 (1987).  
[48] F. M. Nunes and I. J. Thompson, Phys. Rev. C **59**, 2652 (1999).  
[49] J. A. Tostevin, F. M. Nunes, and I. J. Thompson, Phys. Rev. C **63**, 024617 (2001).  
[50] J. Margueron, A. Bonaccorso, and D. M. Brink, Nucl. Phys. **A720**, 337 (2003).  
[51] A. Garcia-Camacho, A. Bonaccorso, and D. M. Brink, Nucl. Phys. **A776**, 118 (2006).  
[52] T. Aumann *et al.*, Phys. Rev. Lett. **84**, 35 (2000).  
[53] C. M. Perey and F. G. Perey, At. Data Nucl. Data Tables **17**, 1 (1976).  
[54] M. Zadro, Phys. Rev. C **70**, 044605 (2004).  
[55] R. Chatterjee, P. Banerjee, and R. Shyam (to be published).  
[56] C. A. Bertulani, H. W. Hammer, and U. van Kolck, Nucl. Phys. **A712**, 37 (2002).